JACS
JOURNAL OF THE AMERICAN CHEMICAL SOCIETY
Communication
pubs.acs.org/JACS

Improved SERS Sensitivity on Plasmon-Free TiO_2 Photonic Microarray by Enhancing Light-Matter Coupling

Dianyu Qi,[†] Liujia Lu,[†] Lingzhi Wang,*[,†] and Jinlong Zhang*[,†,‡]

[†]Key Laboratory for Advanced Materials and Institute of Fine Chemicals, East China University of Science and Technology, 130 Meilong Road, Shanghai 200237, P. R. China

[‡]Department of Chemistry, Tsinghua University, Beijing 100084, P. R. China

Supporting Information

ABSTRACT: Highly sensitive surface-enhanced Raman scattering (SERS) detection was achieved on plasmon-free TiO_2 photonic artificial microarray, which can be quickly recovered under simulated solar light irradiation and repeatedly used. The sensitive detection performance is attributed to the enhanced matter-light interaction through repeated and multiple light scattering in photonic microarray. Moreover, the SERS sensitivity is unprecedentedly found to be dependent on the different light-coupling performance of microarray with various photonic band gaps, where microarray with band gap center near to laser wavelength shows a lower SERS signal due to depressed light propagation, while those with band gap edges near to laser wavelength show higher sensitivity due to slow light effect.

Surface-enhanced Raman scattering (SERS) as a fast and sensitive mean for nondestructive detection of molecules and ions has attracted much attention in analysis, chemistry, and biology fields.[1−4] Because of significant enhancing effect on Raman scattering, Au, Ag, and Cu noble metals have been widely studied and applied in chemicals detection.[5−9] However, the applications of metal substrates are largely limited by their shortcomings such as high-cost, low stability, poor biocompatibility, and no reusability. Photocatalytic self-cleaning SERS substrates have recently been developed by combining plasmonic metal with semiconductor such as TiO_2[10−12] and ZnO,[13,14] which makes SERS substrate recyclable. Actually, semiconductors themselves have proven to be SERS-active.[15−19] However, the development of semiconductor SERS substrate is much underdeveloped compared with metal substrate due to fatal defect of low sensitivity. In spite of this, semiconductor substrates still have drawn considerable attention due to advantages on capability of monitoring and understanding the adsorption behavior of molecules on semiconductor surface, and interference-free detection of metal-catalytically active reaction process.

It is believed that SERS activity of semiconductor is attributed to the charge-transfer (CT) mechanism.[6,20,21] Under the excitation of laser, electrons transfer from semiconductor to adsorbed analytes or from adsorbed analytes to semiconductor. In the CT process, the molecular polarizability is magnified, resulting in enhancement of Raman signals. As a typical semiconductor material, TiO_2 has advantages in stability, economy and biocompatibility.[21−23] However, like other semiconductor SERS substrates, the enhancement factor of TiO_2 is still much lower than that of metal substrate. Whispering gallery mode (WGM) resonance by adopting substrate with cavity can enhance Raman scattering of semiconductor by increasing the reflection of electromagnetic wave in cavity.[24,25] For example, semiconducting carbon nanotubes deposited on Si microarray and SiO_2@TiO_2 core−shell spheres with multiple light scattering resonations have been used to improve SERS detection sensitivity.[26,27] However, SERS substrate based on WGM is still underdeveloped, and the detection sensitivity has great rising potential according to its theoretically expected value.[28]

In the present work, plasmon-free TiO_2 inverse opal photonic microarray was first applied as SERS substrate, which shows unprecedentedly high sensitivity comparable to plasmon metal without the aid of hot spot effect. Photonic semiconductor microarray is well-known for its excellent performance on modulation of light propagation. Although they have long been involved in SERS detection, they were actually only used as carriers for metal particles and have never been used as SERS substrate themselves.[29−36] Here, we report TiO_2 microarray with novel and interesting photonic band gap dependent sensitivity, which can be depressed or improved by careful matching laser wavelength with band gap position. The improved SERS sensitivity here is correlated to the enhanced light-matter interaction in photonic microarray further by comparison study between porous and nonporous film. Moreover, this novel SERS substrate can be easily recovered from instant solar light irradiation and repeatedly used.

TiO_2 inverse opal used in this study was prepared via a simple casting and calcination process, in which close-packed polystyrene (PS) sphere array was used as hard template (Scheme S1). Figure 1a shows Raman spectra of methylene blue (MB) adsorbed on TiO_2 inverse opal (TiO_2-225) and TiO_2 planar. TiO_2 inverse opal shows extraordinary sensitivity in comparison with TiO_2 planar substrate. The detection limit even decreases to 6×10^{-6} M, which is comparable to that of noble metal without the aid of hot spot effect. The intensity of peak at 449 cm^{-1} which ascribed to aggregation reduces with the decreasing concentration, indicating that monomer mainly presents at low concentration and aggregation appears at higher concentration.[36] The inset SEM image indicates TiO_2 inverse

Received: May 26, 2014
Published: June 24, 2014

dx.doi.org/10.1021/ja5052632 | J. Am. Chem. Soc. 2014, 136, 9886−9889

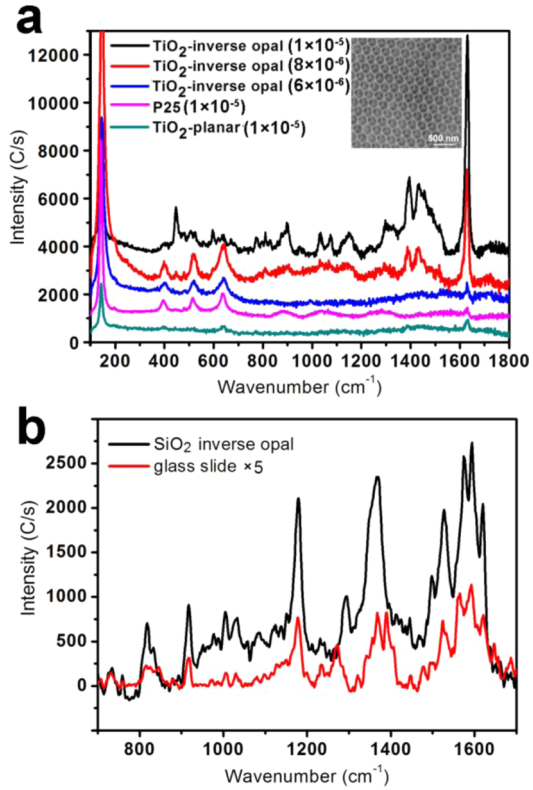

Figure 1. (a) Comparison between Raman spectra of MB with various concentrations adsorbed on TiO_2 inverse opal, TiO_2 planar, and P25. The SEM image of TiO_2 inverse opal is shown in the inset. (b) Raman spectra of 10^{-3} M MB adsorbed on SiO_2 inverse opal substrate and glass slide (multiplied by 5).

opal has highly ordered macroporous structure, which possesses higher specific surface area than TiO_2 planar (Table S2). It cannot be excluded that the enhanced SERS is attributed to the improved specific surface area. Here, P25, a commercial product with specific surface area similar to that of TiO_2 inverse opal, was used as a reference substrate. It is obvious that SERS signal observed from TiO_2 inverse opal is much higher than that of P25 (Figure 1a), which rules out the effect of specific surface area on high SERS sensitivity of TiO_2 inverse opal. However, compared with glass slide, the adsorption and enrichment effect of inverse opal structure with higher specific surface area is still considerable since even non-SERS active substrate of SiO_2 inverse opal shows higher signal intensity than that of glass slide for the detection of 10^{-3} M MB (Figure 1b). The improved signal from TiO_2 inverse opal may be attributed to the repeatedly scattered laser light among the periodic voids. Multiple laser scattering improves light-matter interaction and provides much more opportunities for the occurrence of Raman scattering.

To further prove the effect of improved light-matter coupling in photonic microarray, the macroporous voids in TiO_2 inverse opal were refilled by casting them with TiO_2. It is obvious that the pore size of inverse opal gradually decreases with the casting times, and all of voids fade away after casted thrice (Figure 2a–d). The casting process is illustrated in Figure 2e. TiO_2 precursor solution flows from the top to the bottom of substrate because of gravity, so lower macropores are fully immersed and upper ones are only partly casted by remnant precursor in first two casting processes (middle image in Figure 2e). As a result, the size of upper macropores decreases and

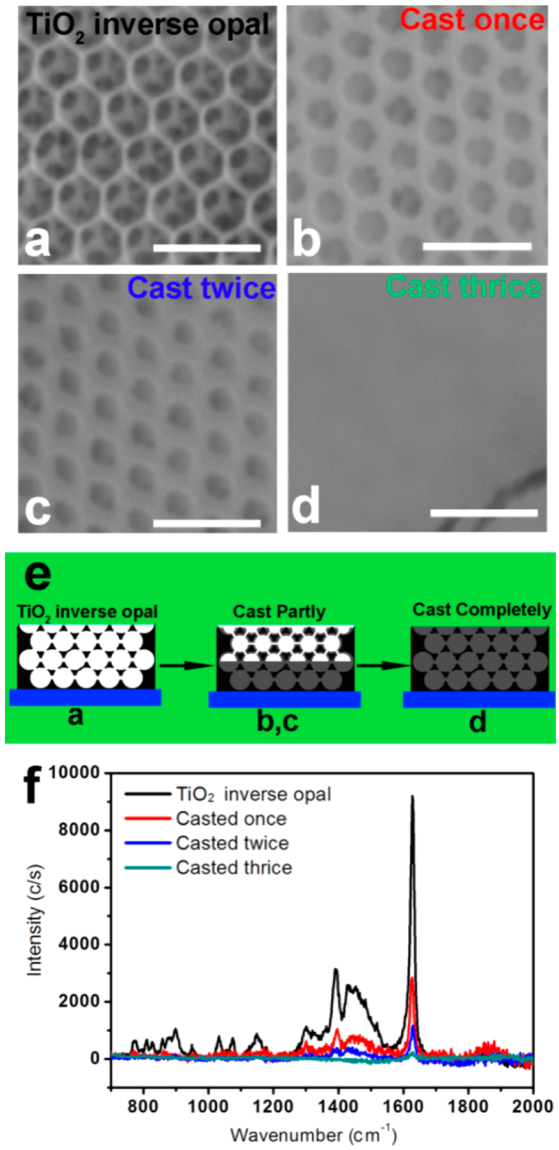

Figure 2. (a–d) SEM images of TiO_2 inverse opal casted 0, 1, 2, and 3 times (the scale bar is 500 nm); (e) scheme of casting process; (f) Raman spectra of 10^{-5} M MB adsorbed on the substrates casted 0, 1, 2, and 3 times.

voids in the bottom of substrate completely disappear after hydrolysis and calcination treatment. The macropores are completely filled when efficient precursor solution is used (right image in Figure 2e). Raman spectra of MB on casted samples indicate the intensity significantly decreases with the casting times (Figure 2f). The Raman signal observed from the sample losing multiple light scattering properties is as low as that of TiO_2 planar. Therefore, the efficient light-matter coupling by multiple light scattering actually plays a determinative role in the sensitive SERS detection.

Inverse opal as a kind of photonic crystal has photonic band gap in a certain wavelength, meaning that the propagation of light at this wavelength is theoretically forbidden, and the propagation of light at the edge of the photonic band gap can be slowed down.[37] Therefore, the SERS detection performance of TiO_2 inverse opal is probably related to the position of photonic band gap. Subsequently, TiO_2 inverse opals with different photonic band gap were prepared to investigate the

dx.doi.org/10.1021/ja5052632 | J. Am. Chem. Soc. 2014, 136, 9886–9889

effect of photonic band gap on SERS activity. The band gap position is tuned by adjusting the size of macropore. Figure 3a–d is SEM images of TiO_2 inverse opals with different void

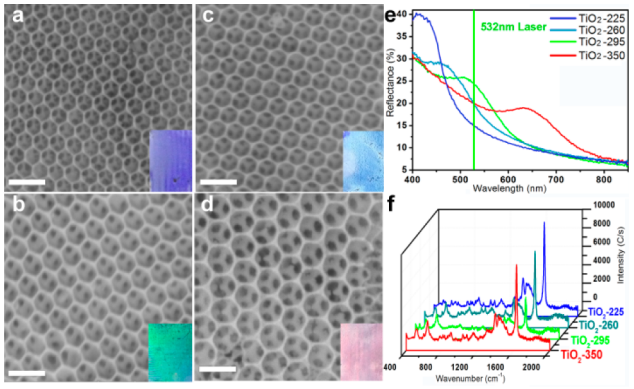

Figure 3. (a–d) SEM images of TiO_2 inverse opal substrates (TiO_2-225, TiO_2-260, TiO_2-295, and TiO_2-350), and the scale bar is 500 nm. The insets are photographs of the substrates under white light irradiation. (e) Reflection spectra of TiO_2 inverse opal substrates. (f) Raman spectra of 10^{-5} M MB adsorbed on different inverse opal substrates.

sizes including 225, 260, 295, and 350 nm. As shown in the insets, TiO_2 inverse opals show different colors because of the various photonic band gaps. Reflection spectra were measured (Figure 3e) to estimate the positions of band gaps. The photonic band gaps of TiO_2-350, 295, 260, and 225 are around 650, 530, 470, and 420 nm, respectively. The band gap positions obviously match well with the colors of the inverse opal substrates. The wavelength of laser applied in this study is 532 nm, which locates in the center of the photonic band gap of TiO_2-295 substrate and at the edge of the photonic band gap of TiO_2-225. Therefore, multiple light scattering should be suppressed in the case of TiO_2-295 due to the photonic forbidden band and enhanced in the case of TiO_2-225 due to slow light effect.[38]

Raman spectra of 10^{-5} M MB adsorbed on various substrates are shown in Figure 3f. Significant variation in the intensity is observed although all of substrates have no chemical difference, indicating that diversity in SERS should be attributed to the position of photonic band gap. Samples TiO_2-225 and TiO_2-295 show highest and lowest sensitivity, respectively. In the case of TiO_2-225, multiple-light scattering of the laser is maximized because of slow light effect, resulting in the highest intensity of Raman spectrum. The decreased SERS effect in other samples should be attributed to weakened light-mattering interaction in the absence of slow light effect and the lowest sensitivity of TiO_2-295 substrate should be attributed to its band gap close to laser light, where the propagation of laser and multiple scattering is largely suppressed. The propagation of laser is suppressed rather than forbidden because of the existence of defects in TiO_2 inverse opals prepared by colloidal deposition method.

Because of intrinsic self-clean ability of TiO_2, TiO_2 inverse opal substrate can decompose organic analyte under solar light irradiation. Photodegradation of 10^{-5} M MB on TiO_2 inverse opal substrate was tested under simulated sunlight irradiation (Figure 4a). After 5 min irradiation, few peaks of MB remain, and all peaks of MB disappear after 10 min irradiation, indicating that MB is completely photodegraded. The substrate

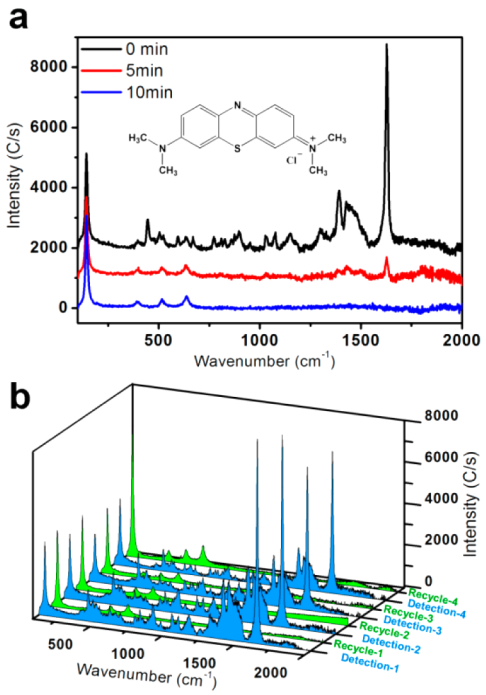

Figure 4. (a) Raman spectra of 10^{-5} M MB adsorbed on TiO_2 inverse opal substrate under simulated sunlight irradiation for different times (0, 5, and 10 min). (b) Recycle experiment test of TiO_2 inverse opal substrate. The initial concentration of MB is 10^{-5} M, and the simulated sunlight irradiation time is 10 min.

also shows well self-cleaning ability when higher concentration MB is adsorbed (Figure S2). The rapid and efficient self-cleaning ability may also be attributed to the improved light-harvesting ability of TiO_2 inverse opal. Recycling experiment was further done to test the stability of the substrate (Figure 4b), and the substrate still shows excellent SERS activity after three runs of circulation.

Subsequently, the enhancement factor (EF) of the TiO_2 inverse opal substrate is evaluated by eq 1.[39−42] N_{SERS} and N_0 are the average number of molecules in scattering area for SERS and non-SERS measurement, and I_{SERS} and I_0 are the intensities of the selected Raman peak in the SERS and non-SERS spectra. In this study, the numbers of probe molecules were estimated by eq 2 on the assumption that the probed molecules were distributed uniformly on the substrates.[10] N_A is Avogadro constant, C is the molar concentration of the probed solution, V is the volume of the droplet, S_{scan} is the area of Raman scanning, and S_{sub} is the area of the substrate. The Raman spectra of MB adsorbed on SERS and non-SERS substrates are shown in Figure S3, and the calculated EF is 2.0×10^4, which is outstanding sensitivity for plasmon-free TiO_2 substrates.

$$\mathrm{EF} = \frac{I_{SERS}/N_{SERS}}{I_0/N_0} \quad (1)$$

$$N = CVN_A S_{scan}/S_{sub} \quad (2)$$

In conclusion, plasmon-free TiO_2 inverse opals SERS substrates were fabricated, and high sensitive detection was achieved due to the improved light-mattering coupling. The detection sensitivity is governed by the position of photonic band gap, where the highest sensitivity can be achieved by appropriately utilizing slow light effect of photonic microarray. Moreover, TiO_2 inverse opal also shows an outstanding

dx.doi.org/10.1021/ja5052632 | J. Am. Chem. Soc. 2014, 136, 9886–9889

recyclability by optical irradiation, which should also be attributed to their efficient light-harvesting ability.

■ ASSOCIATED CONTENT

Supporting Information

Experimental details, including XRD patterns, Raman spectra of MB adsorbed on SERS and none SERS, and BET surface area. This material is available free of charge via the Internet at http://pubs.acs.org.

■ AUTHOR INFORMATION

Corresponding Authors

wlz@ecust.edu.cn
jlzhang@ecust.edu.cn

Notes

The authors declare no competing financial interest.

■ ACKNOWLEDGMENTS

This work has been supported by the National Nature Science Foundation of China (21173077, 21377038 and 21237003, 21203062), the National Basic Research Program of China (973 Program, 2013CB632403), the Science and Technology Commission of Shanghai Municipality (12230705000, 12XD1402200), the Research Fund for the Doctoral Program of Higher Education (20120074130001) and the Fundamental Research Funds for the Central Universities.

■ REFERENCES

(1) Ni, J.; Lipert, R. J.; Dawson, G. B.; Porter, M. D. *Anal. Chem.* **1999**, *71*, 4903.
(2) Wang, Z.; Zong, S.; Li, W.; Wang, C.; Xu, S.; Chen, H.; Cui, Y. *J. Am. Chem. Soc.* **2012**, *134*, 2993.
(3) Qian, X.; Li, J.; Nie, S. *J. Am. Chem. Soc.* **2009**, *131*, 7540.
(4) Sharma, B.; Ma, K.; Glucksberg, M. R.; Van Duyne, R. P. *J. Am. Chem. Soc.* **2013**, *135*, 17290.
(5) Fleischmann, M.; Hendra, P. J.; McQuillan, A. *J. Chem. Phys. Lett.* **1974**, *26*, 163.
(6) Wang, X.; Shi, W.; She, G.; Mu, L. *Phys. Chem. Chem. Phys.* **2012**, *14*, 5891.
(7) Zhu, Y.; Kuang, H.; Xu, L.; Ma, W.; Peng, C.; Hua, Y.; Wang, L.; Xu, C. *J. Mater. Chem.* **2012**, *22*, 2387.
(8) Zhao, J.; Jensen, L.; Sung, J.; Zou, S.; Schatz, G. C.; Van Duyne, R. P. *J. Am. Chem. Soc.* **2007**, *129*, 7647.
(9) Allen, C. S.; Van Duyne, R. P. *J. Am. Chem. Soc.* **1981**, *103*, 7497.
(10) Li, X.; Hu, H.; Li, D.; Shen, Z.; Xiong, Q.; Li, S.; Fan, H. J. *ACS Appl. Mater. Interfaces* **2012**, *4*, 2180.
(11) Tan, E.-Z.; Yin, P.-G.; You, T.-t.; Wang, H.; Guo, L. *ACS Appl. Mater. Interfaces* **2012**, *4*, 3432.
(12) Jiang, X.; Li, X.; Jia, X.; Li, G.; Wang, X.; Wang, G.; Li, Z.; Yang, L.; Zhao, B. *J. Phys. Chem. C* **2012**, *116*, 14650.
(13) Sinha, G.; Depero, L. E.; Alessandri, I. *ACS Appl. Mater. Interfaces* **2011**, *3*, 2557.
(14) Mao, Z.; Song, W.; Chen, L.; Ji, W.; Xue, X.; Ruan, W.; Li, Z.; Mao, H.; Ma, S.; Lombardi, J. R. *J. Phys. Chem. C* **2011**, *115*, 18378.
(15) Tarakeshwar, P.; Finkelstein-Shapiro, D.; Hurst, S. J.; Rajh, T.; Mujica, V. *J. Phys. Chem. C* **2011**, *115*, 8994.
(16) Xue, X.; Ji, W.; Mao, Z.; Mao, H.; Wang, Y.; Wang, X.; Ruan, W.; Zhao, B.; Lombardi, J. R. *J. Phys. Chem. C* **2012**, *116*, 8792.
(17) Maznichenko, D.; Venkatakrishnan, K.; Tan, B. *J. Phys. Chem. C* **2012**, *117*, 578.
(18) Teguh, J. S.; Liu, F.; Xing, B.; Yeow, E. K. *Chem. Asian J.* **2012**, *7*, 975.
(19) Maznichenko, D.; Selvaganapathy, P.; Venkatakrishnan, K.; Tan, B. *Appl. Phys. Lett.* **2012**, *101*, 231602.
(20) Yang, L.; Jiang, X.; Ruan, W.; Zhao, B.; Xu, W.; Lombardi, J. R. *J. Phys. Chem. C* **2008**, *112*, 20095.
(21) Musumeci, A.; Gosztola, D.; Schiller, T.; Dimitrijevic, N. M.; Mujica, V.; Martin, D.; Rajh, T. *J. Am. Chem. Soc.* **2009**, *131*, 6040.
(22) Yang, L.; Jiang, X.; Ruan, W.; Zhao, B.; Xu, W.; Lombardi, J. R. *J. Raman Spectrosc.* **2009**, *40*, 2004.
(23) Kiran, V.; Sampath, S. *ACS Appl. Mater. Interfaces* **2012**, *4*, 3818.
(24) White, I. M.; Hanumegowda, N. M.; Oveys, H.; Fan, X. *Opt. Express* **2005**, *13*, 10754.
(25) Arnold, S.; Keng, D.; Shopova, S.; Holler, S.; Zurawsky, W.; Vollmer, F. *Opt. Express* **2009**, *17*, 6230.
(26) Sumikura, H.; Kuramochi, E.; Taniyama, H.; Notomi, M. *Appl. Phys. Lett.* **2013**, 102.
(27) Alessandri, I. *J. Am. Chem. Soc.* **2013**, *135*, 5541.
(28) Ausman, L. K.; Schatz, G. C. *J. Chem. Phys.* **2008**, *129*, 054704.
(29) Kuncicky, D. M.; Prevo, B. G.; Velev, O. D. *J. Mater. Chem.* **2006**, *16*, 1207.
(30) TongáLee, S. *J. Mater. Chem.* **2012**, *22*, 1370.
(31) Mu, W.; Hwang, D.-K.; Chang, R. P. H.; Ketterson, J. B. *J. Raman Spectrosc.* **2011**, *42*, 941.
(32) Tessier, P. M.; Velev, O. D.; Kalambur, A. T.; Lenhoff, A. M.; Rabolt, J. F.; Kaler, E. W. *Adv. Mater.* **2001**, *13*, 396.
(33) Tessier, P. M.; Velev, O. D.; Kalambur, A. T.; Rabolt, J. F.; Lenhoff, A. M.; Kaler, E. W. *J. Am. Chem. Soc.* **2000**, *122*, 9554.
(34) Kuncicky, D. M.; Christesen, S. D.; Velev, O. D. *Appl. Spectrosc.* **2005**, *59*, 401.
(35) Velev, O. D.; Kaler, E. W. *Adv. Mater.* **2000**, *12*, 531.
(36) Alessandri, I.; Ferroni, M. *J. Mater. Chem.* **2009**, *19*, 7990.
(37) Stein, A.; Wilson, B. E.; Rudisill, S. G. *Chem. Soc. Rev.* **2013**, *42*, 2763.
(38) Krauss, T. F.; Rue, R. M. D. L.; Brand, S. *Nature* **1996**, *383*, 699.
(39) Lal, S.; Grady, N. K.; Goodrich, G. P.; Halas, N. J. *Nano Lett.* **2006**, *6*, 2338.
(40) McFarland, A. D.; Young, M. A.; Dieringer, J. A.; Van Duyne, R. P. *J. Phys. Chem. B* **2005**, *109*, 11279.
(41) Le Ru, E.; Blackie, E.; Meyer, M.; Etchegoin, P. G. *J. Phys. Chem. C* **2007**, *111*, 13794.
(42) Hu, Y.; Shi, Y.; Jiang, H.; Huang, G.; Li, C. *ACS Appl. Mater. Interfaces* **2013**, *5*, 10643.